An Effective 3-D Solver for MMIC Interconnects – EVFE Technique with PML

Weijun Yao and Yuanxun Wang
Department of Electrical Engineering, University of California at Los Angeles,
405 Hilgard Avenue, Los Angeles, CA90095-1594, U.S.

Abstract **— In this paper, the perfectly matched layer boundary condition has been successfully implemented into the 3-D envelope finite element (EVFE) techniques to truncate the space meshes. The numerical test shows that PML can provide 40dB overall absorption in the presence of four layers of absorber. A few MMIC interconnect structures were analyzed using EVFE techniques with PML boundary conditions. The results demonstrate that the proposed approach is an efficient and precise way to analyze the MMIC interconnects.**

I. INTRODUCTION

Recently a novel technique called envelope finite element (EVFE) has been proposed to simulate the time-domain envelopes of electromagnetic waves [1-4]. It has been demonstrated that EVFE technique is computationally efficient for both narrow band and broadband problems. Therefore, it will be a powerful simulator for high speed circuit design in wireless or optical communication such as Monolithic-Microwave Circuits (MMIC).

One previous limitation for the applicability and efficiency of the EVFE technique is the boundary condition used to terminate the space meshes. In [1], the first order ABC boundary condition is applied to 2-D EVFE in parallel waveguide structures. The ABC formulations for 3-D EVFE have also been derived in [3][4] to solve 3-D waveguide discontinuity problems and for microstrip circuits analysis. Though an easy implementation, the performance of the ABC will be severely degraded when the signal bandwidth increases. The better choice is to truncate the EVFE meshes with a perfectly matched layer (PML) which has strong absorption and wide bandwidth. A 2-D implementation of PML is proposed in [2], which exhibits good absorption to the EM waves with different incident angles in a parallel waveguide.

In this paper, we will derive the 3-D PML formulation for EVFE technique. The performance of PML is tested numerically, showing 40dB absorption when four layers of PML are used. Two MMIC structures are analyzed to demonstrate the high efficiency and accuracy of the proposed approach.

This paper is organized as follows. Section II presents the 3-D EVFE formulation implementing the anisotropic PML. One numerical example is presented to test the validity of the formulations. In section III, we use EVFE with PML to analyze two 3-D MMIC interconnect structures. Finally, conclusions are drawn in Section IV.

II. PML FOR EVFE FORMULATION

The derivation for 3-D EVFE-PML formulation is similar as the 2-D case in [2]. We still start from the general time-harmonic form of Maxwell equations in PML regions:

$$\nabla\times\vec{H} = j\omega\varepsilon_0\varepsilon_r\bar{\bar{\varepsilon}}\vec{E} + \vec{J}_i$$
$$\nabla\times\vec{E} = -j\omega\mu_0\mu_r\bar{\bar{\mu}}\vec{H} \qquad (1)$$

Where

$$\bar{\bar{\varepsilon}} = \bar{\bar{\mu}} = \begin{bmatrix} \frac{s_y s_z}{s_x} & 0 & 0 \\ 0 & \frac{s_x s_z}{s_y} & 0 \\ 0 & 0 & \frac{s_x s_y}{s_z} \end{bmatrix} \qquad (2)$$

and $$s_i = 1 + \frac{\sigma_i}{j\omega\varepsilon_0} \quad , i = x, y, z \qquad (3)$$

Here we assume there is no source in PML region, and the second-order wave equation from (1), (2), and (3) is as:

$$\nabla\times\left(\left[\bar{\bar{\mu}}\right]^{-1}\cdot\nabla\times\vec{E}\right) - \omega^2\varepsilon\left[\bar{\bar{\varepsilon}}\right]\vec{E} = -j\omega\frac{1}{\mu}\vec{J} \qquad (4)$$

Based on the vector finite element method, we can recast the equation (4) into the following form:

$$-\omega^2 e_j Q_x \frac{s_y s_z}{s_x} + e_j P_x \frac{s_x}{s_y s_z} - \omega^2 e_j Q_y \frac{s_x s_z}{s_y} + e_j P_y \frac{s_y}{s_x s_z}$$
$$-\omega^2 e_j Q_z \frac{s_y s_x}{s_z} + e_j P_z \frac{s_z}{s_y s_z} = -j\omega\int_v \frac{1}{\mu}\overline{N}_i \bullet \vec{J} dv \qquad (5)$$

Where

0-7803-7695-1/03/$17.00 © 2003 IEEE

$$Q_x = \int_v \varepsilon N_x^j N_x^i dv \quad Q_y = \int_v \varepsilon N_y^j N_y^i dv$$

$$Q_z = \int_v \varepsilon N_z^j N_z^i dv \quad P_x = \int_v \frac{1}{\mu}(\nabla\times\vec{N}^j)_x(\nabla\times\vec{N}^j)_x dv$$

$$P_y = \int_v \frac{1}{\mu}(\nabla\times\vec{N}^j)_y(\nabla\times\vec{N}^j)_y dv$$

$$P_z = \int_v \frac{1}{\mu}(\nabla\times\vec{N}^j)_z(\nabla\times\vec{N}^j)_z dv \qquad (6)$$

$\vec{N}^i, \vec{N}^j$ are the vector basis functions.

To solve equation (5), we need to define another three variables:

$$\Phi_x = \frac{s_x}{s_y s_z} e_j \quad \Phi_y = \frac{s_y}{s_x s_z} e_j$$

$$\Phi_z = \frac{s_z}{s_x s_z} e_j \qquad (7)$$

Equation (3-5) is reduced to:

$$-\omega^2\Phi_z Q_x s_y^2 + P_x\Phi_x - \omega^2\Phi_x Q_y s_z^2 + P_y\Phi_y$$

$$-\omega^2\Phi_z Q_z s_x^2 + P_z\Phi_z = -j\omega\int_v \frac{1}{\mu}\vec{N}\bullet\vec{J}dv \qquad (8)$$

And defining the signal envelope as:

$$\begin{aligned} e_j(t) &= u_j(t)e^{j\omega_c t} \\ \Phi_j(t) &= \psi_j(t)e^{j\omega_c t} \\ J_z(t) &= j_z(t)e^{j\omega_c t} \end{aligned} \qquad (9)$$

Substitute (9) into (8) we can obtain the differential equation about the signal envelope:

$$Q_x\frac{d^2\psi_z}{dt^2} + [S_1]\frac{d\psi_z}{dt} + [S_2]\psi_z + Q_y\frac{d^2\psi_x}{dt^2}$$
$$+ [S_3]\frac{d\psi_x}{dt} + [S_4]\psi_x + Q_z\frac{d^2\psi_y}{dt^2} + [S_5]\frac{d\psi_y}{dt}$$
$$+ [S_6]\psi_y = -(\frac{\partial f_i}{\partial t} + j\omega_c f_i) \qquad (10)$$

Where

$$S_1 = 2(j\omega_c + \frac{\sigma_y}{\varepsilon_0}) \quad S_2 = (j\omega_c + \frac{\sigma_y}{\varepsilon_0})^2 Q_x + P_z$$

$$S_3 = 2(j\omega_c + \frac{\sigma_z}{\varepsilon_0}) \quad S_4 = (j\omega_c + \frac{\sigma_z}{\varepsilon_0})^2 Q_y + P_x$$

$$S_5 = 2(j\omega_c + \frac{\sigma_x}{\varepsilon_0}) \quad S_6 = (j\omega_c + \frac{\sigma_x}{\varepsilon_0})^2 Q_z + P_y$$

$$f_i = \int_v \frac{1}{\mu}\overline{N_i}\bullet\vec{J}dv \qquad (11)$$

Using Newmark-Beta formulation to descretize (10), we can obtain the time recursive formulation:

$$R_1\psi_z^{n+1} + R_2\psi_z^n + R_3\psi_z^{n-1} + R_4\psi_x^{n+1} + R_5\psi_x^n + R_6\psi_x^{n-1} + R_7\psi_y^{n+1}$$
$$+ R_8\psi_y^n + R_9\psi_y^{n-1} = -(\frac{f_i^{n+1} - f_i^{n-1}}{2\Delta t} + j\omega_c\frac{f_i^{n+1} + 2f_i^n + f_i^{n-1}}{4}) \qquad (12)$$

Where R_i are the coefficient matrixes. According to (7), we can obtain the relationship between the ψ_ξ (ξ=x,y,z) and u with Newmark-Beta formulation:

$$\psi_\xi^{n+1} = a_{\xi 5}\psi_\xi^n + a_{\xi 6}\psi_\xi^{n-1} + a_{\xi 7}u^{n+1} + a_{\xi 8}u^n + a_{\xi 9}u^{n-1} \qquad (13)$$

Where ξ=x,y,z and $a_{\xi i}$ are the complex coefficients. Combining equation (12) and (13), and solving them, the complex signal envelope vectors $u=[u_1,u_2,...,u_N]$ and $\Psi_\xi = [\Psi_{\xi 1}, \Psi_{\xi 2}, ..., \Psi_{\xi N}]$ can be solved in time domain.

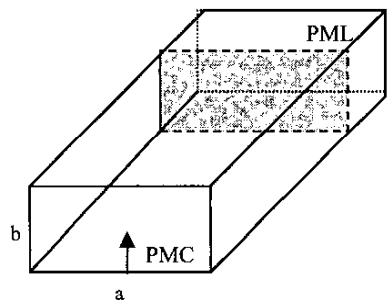

Fig. 1 Rectangle Waveguide with PML set at one end, and PMC set at the other end. The crossection is 10.16mm*22.86mm

To evaluate the performance of the PML, the PML medium was set in the z direction at the end of the rectangle waveguide (see Fig.1). The other end is terminated by a PMC and we can set the excitation on this PMC (z=0) to test the reflection from PML at the other end. The mesh size along z direction is 2mm, which is about 8.6% of the smallest wavelength. In order to reduce the discretization error, we use spatially variant conductivity along the normal axis [5-6]:

$$\sigma_z(z) = \frac{\sigma_{\max}|z - z_0|^m}{\sqrt{\varepsilon_r}\,d^m} \qquad (14)$$

Where z_0 is the interface between the PML region and non-PML region, d is the depth of the PML and m is the order the polynomial variation. The order m=2 is chosen for better absorption.

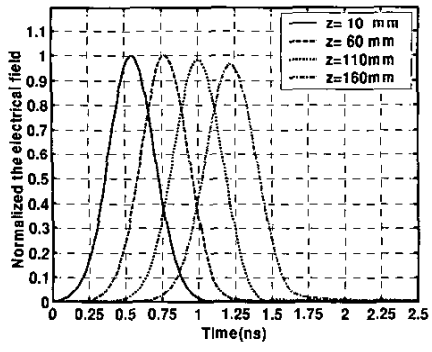

Fig.2 wave envelopes propagates in the empty waveguide

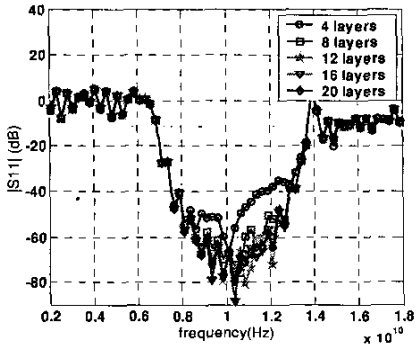

Fig.3 Reflection error of PML with varying number of layers.

Fig. 2 shows the time domain wave envelopes in this waveguide. The four waveforms represent the normalized electrical fields in four fixed positions z=10mm, 60mm, 110mm, 160mm. The four Gaussian envelopes distort as the wave propagates along the waveguides. This distortion in the wave envelopes is caused by dispersive character of the rectangle waveguide, whose domain mode is TE_{10} mode.

Fig. 3 shows the magnitude of S_{11} with varying depths of PML with variant σ_{max}. The excitation's bandwidth is 4GHz and the center frequency is 10 GHz. The result indicates that the larger the PML depth is, the better the PML performs. When we set the PML to more than four layers, we can easily get a reflection lower than -40dB.

III. ANAYLISIS MMIC STRUCTURES WITH EVFE_PML TECHNIQUE

Two numerical examples about MMIC structures will be presented here.

A vertical metallic via hole in the dielectric substrate is widely used in modern MMIC design. It provides a short circuit or feeding point for the RF signals, thus it becomes a vital component in the MMIC structures [8][10].

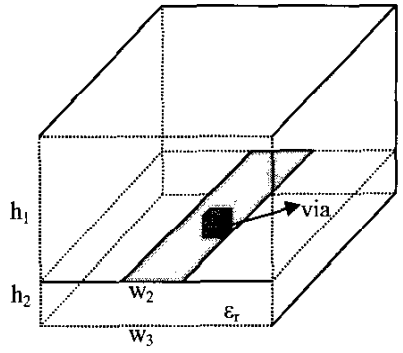

Fig. 4 Geometry of microstrip grounded via

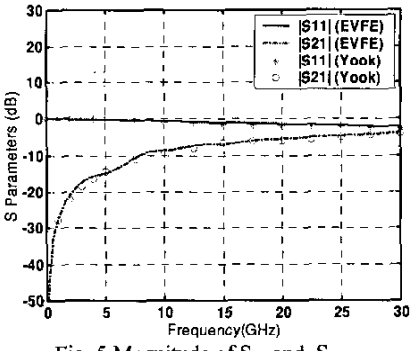

Fig. 5 Magnitude of S_{11} and S_{21}

Fig. 4 shows a chip-level grounded via in a microstrip line printed on a GaAs substrate (ε_r=12.9). The sizes of this structure are: h1=250μm, h2=600μm, w2=600μm, w3=1785μm. Here we assume that the via has a square crossection with the size 85μm. The two sides, bottom and top surfaces are PEC walls. The front and end are truncated by PML absorbers. In this example, we want to show EVFE_PML technique's broadband simulation performance (from 0GHz to 30GHz), thus we set the carrier frequency as 15GHz with the excitation's bandwidth as 15GHz. The time step is 2ps, which is about 4 times sparser than that required by regular FETD. The PML depth is about 5000μm. The magnitude of S_{11} and S_{21} are plotted in Fig.5, and the results agree very well with Yook's [8].

The second example is two microstrip lines joined with an air or dielectric bridge, as depicted in Fig. 6. The microstrip line has a width a and a thickness 0.2a, which is printed on GaAs substrate (ε_{r1}=12.9). The bridge has a length 12.7a with the dielectric constant ε_{r2}. Like the previous example, the structure is closed by PEC walls

except that the front and end are terminated by PML absorbers. In EVFE formulations, we set the center frequency is according to k_0a=0.24 and set the bandwidth according to k_0a=0.12, where k_0 is the wave number in free space. The PML depth is about 4a. The magnitude of S_{11} is shown in Fig.7, versus different ε_{r2}. The results are also compared to those of the frequency domain finite difference method [9], and they agree with each other very well.

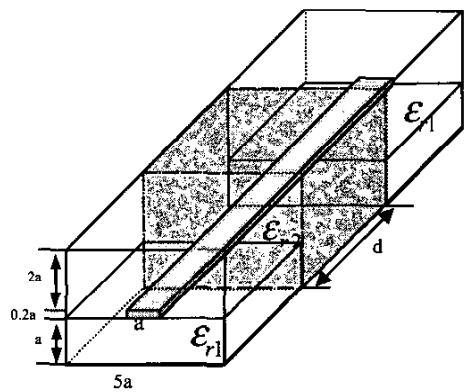

Fig. 6 Geometry of air or dielectric bridge in MMICs

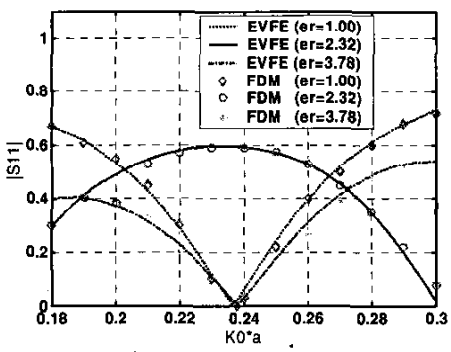

Fig. 7 Magnitude of S_{11}

IV. CONCLUSION

In this paper, anisotropic PML has been implemented into the 3-D EVFE algorithm. One numerical example of an empty rectangle waveguide has been presented to evaluate the PML's performance and more than 40dB absorption is achieved when a 4-layer absorber is set. The EVFE-PML technique is validated through the simulation of the two MMIC structures. As a result, other 3-D problems such as antenna scattering problems can also be easily solved with the EVFE-PML technique

ACKNOWLEDGEMENT

The authors would like to than Dr. D. Jiao for helpful discussions in 2002 Antenna and Propagation Symposium and Katie Allen for the language improvement for this paper.

REFERENCES

[1] Yuanxun Wang and Tatsuo Itoh, "Envelope-finite element(EVFE) Technique – A more efficient time domain scheme", *IEEE Trans. Microwave Theory Tech.* Dec. 2001.

[2] Weijun Yao, Y. Wang, "Envelope-finite element (EVFE) technique for electromagnetics in general media", submitted *to IEEE Trans. on Antennas Propagat.*

[3] Hsiao-Ping Tsai,Yuanxun Wang and Tatsuo Itoh, Efficient analysis of microwave passive structures using 3-D envelope-finite element (EVFE)", *IEEE Trans. Microwave Theory Tech.* Volume: 50 Issue: 12 , Dec. 2002, pp2721 - 2727.

[4] A. Frasson and H. E Hemandez Figueroa, "Envelope Gull-Wave 3D Finite Element Time Domain Method", *Microwave and Optical Technology Letters*, pp351-354, Vol. 35, No. 5, Dec. 5, 2002

[5] S.D. Gedney, "An Anisotropic Perfectly Matched Layer Absorbing Medium for the Truncation of FDTD Lattices," *IEEE Trans. Antennas Propagat.*, vol.44, (no.12),pp.1630-1639, Dec. 1993.

[6] Hsiao-Ping Tsai, Yuanxun Wang and Tatsuo Itoh, "An Unconditionally Stable Extended (USE) Finite Element Time Domain Solution of Active Nonlinear Microwave Circuits Using Perfectly Matched Layers", *IEEE Trans. Microwave Theory Tech.* Oct. 2002, pp2226 -2232.

[7] D. Jiao, J. M. Jin, E. Michielessen, and D. Riley "Time domain finite-element simulation of three-dimensional scattering and radiation problems using perfectly matched layers", *2002 IEEE AP-S,* volume 2.pp158-161.

[8] J.G. Yook, N. I. Dib and L. P. B. Katehi, "Characterization of high frequency interconnects using finite difference time domain and finite element methods",*IEEE Trans. Microwave Theory Tech.*, vol. 42, pp.1727-1736, Sept. 1994.

[9] A. Christ and H. L. Hartnagel, "Three-dimensional finite difference method for the analysis of microwave-device embedding", *IEEE Trans. Microwave Theory Tech.*, vol. 35, pp.688-696, Aug. 1987.

[10] Yongxi Qian and Tatsuo Itoh, "FDTD analysis and design of microwave circuits and antennas- software and applications" ,1999